

Supporting Information for

Quinone-Fused Porphyrins as Contrast Agents for Photoacoustic Imaging

Srinivas Banala,^{*a,b} Stanley Fokong,^a Christian Brand,^c Chrysafis Andreou,^c Bernhard Kräutler,^d Magnus Rueping,^b and Fabian Kiessling^a

^a Experimental Molecular Imaging, University Clinic, RWTH Aachen University, D-52074 Aachen, Germany. E-mail: sbanala@ukaachen.de

^b Institute of Organic Chemistry, RWTH Aachen University, Landoltweg 1, Germany.

^c Department of Radiology, Memorial Sloan Kettering Cancer Centre, 10065 New York; USA.

^d Institute of Organic Chemistry, University of Innsbruck, Innrain 80-82, Innsbruck, Austria.

Contents:

1. General	S2
2. Photoacoustic imaging	S2
Calculation of relative PA intensity	S2
3. XTT-cell viability assay	S3
4. <i>In vivo</i> multi-spectral photoacoustic imaging (MSOT)	S3
5. Metal insertions into black metal-free porphyrins	S4
A) Synthesis of black Co ^(II) Porphyrin (3-Co)	
B) Synthesis of black Cu ^(II) Porphyrin (3-Cu)	
C) Tetranaphthoquinono Porphyrins 3-Zn , 3-Ni , 3-2H	
6. UV/Vis spectra	S7
7. Fluorescence Emission of 3-Zn	S8
8. Phantom design images	S9
9. PA spectroscopy	S10
10. Stability of 3-Zn in 10% fetal calf serum (FCS)	S14
11. Stability of 3-Zn to excess of free thiol (N-Ac-Cys-OMe)	S16
12. MS spectra	S18
13. References	S19

1. General.

All the reactions, work-up and chromatography were performed under protection from light (wrapping in alumina foil). All the glassware for the reactions was oven dried at 100 °C and cooled under high vacuum (HV) before use and kept under argon. Absolute solvents were prepared by distillation over calcium hydride. Organic solutions were concentrated under reduced pressure on a Büchi rotary evaporator (< 37°C water bath). Thin-layer chromatography was carried out using Merck Kieselgel 60 F254 (230-400 mesh, 25x25cm for preparative scale). Solvents - dichloromethane (CH₂Cl₂), ethylacetate (EtOAc), and hexane were distilled before use from technical grade solvents. Methanol from Acros HPLC grade, Cu(OAc)₂.H₂O (> 99% purity) from Merck, and anhydrous CoBr₂ from Acros (>99% purity) are used as received. UV/Vis spectra: *PerkinElmer Lambda 35 spectrometer*, in 10mm quartz cells, λ_{\max} (log ϵ) in nm. Fluorescence spectra: *PerkinElmer LS45* or *Varian Cary Eclipse*. MS: MALDI (DHB matrix, Bruker Ultraflex MALDI TOF (Bruker Daltonic GmbH), m/z (rel. intensity %).

2. Photoacoustic Imaging: The pre-clinical PA device VEVO LAZR (from Visualsonics Inc, Amsterdam, NL) equipped with a LZ 250 transducer having a centre frequency of 21 MHz was used for scanning (26 db gain). The VEVO LAZR built-in pulse laser (wavelengths between 680-970 nm) was warmed up for 30 min before use and energy was calibrated using an internal sensor. Tube phantom experiments were carried at 9-11 mm depth in a water chamber with total of 59 (for 5 nm step) or 146 frames (2 nm steps). The Vevo 2100 software was used for data processing. During the measurements of serial dilutions, all variable parameters were kept constant i.e. photoacoustic gain, laser power, focus depth, frame averaging, and frame rate.

Calculation of relative photoacoustic intensity:

PA intensity (a.u) was measured in tube phantoms for all the solutions using identical regions of interest. The PA Avg signal/conc ratios of the black porphyrins were divided by the according ratio of ICG (then, for ICG relative PA intensity becomes 1).

3. Cell Viability XTT assay

In a 96-well plate, A549 cells (5×10^3 to 10×10^3) were seeded and treated with DMEM media supplemented with 10% FCS, 1% penicillin/streptomycin (P/S). The cells were incubated at 37 °C (in 5% CO₂ incubator) for 24 h to let the cells attach to the surface of the 96-well plate. The substance in DMEM media (conc. 0.001 μmol/ml to 0.1 μmol/ml) was added to the above well plate, and further incubated at 37 °C in 5% CO₂ incubator for 24 h. XTT-solution was freshly prepared by XTT test kit (using the prescribed protocol from Gibco), and 50 μL of this mixture was added to each well of the above cells. After 2-4 h, the absorption was measured in TECAN-reader at 475 nm wavelength using 660 nm as reference.

4. *In vivo* multi-spectral optoacoustic imaging (MSOT)

Two dimensional (2D) static multispectral optoacoustic (MSOT) imaging was performed on a previously described inVision 256-TF system from iThera Medical (Munich, Germany) [S1, S2]. Female nude mice (4-6 weeks, n = 6, performed according to the Guidelines for the Care and Use of Animals for Research, approved by MSKCC's Institutional Animal Care and Use Committee) were intravenously injected with **3-Zn** (150 μL, 100 μM, 30% PEG300 in PBS, n=3) and PBS (150 μL, n=3). At 1 h post injection, mice were euthanized by asphyxiation with CO₂. Blood was collected via cardiac puncture and selected organs, liver, kidney, and muscle, were harvested for *ex vivo* MSOT imaging. Wavelengths from 700 nm to 900 nm in 20 nm steps (power: 100 mW) were used for excitation, with 5 acquisitions averaged per wavelength per frame. After image reconstruction, linear spectral unmixing was conducted to detect and select the specific signal of 'black' porphyrin from other intrinsic signal such as oxygenated and deoxygenated hemoglobin. All images were scaled to the same threshold (arbitrary units) to compare tissue injected with black porphyrin from PBS. To quantify the signal, the black porphyrin channel (green) was averaged over a circular area at the slices central to each tissue.

5. Metal insertions into black metal-free porphyrins

A) *Tetranaphthoquinono Copper^(II) Porphyrin (3-Cu)*: In dry 10 mL round bottomed flask, 1.8 mg of (1.14 μmol) **3-2H** was taken under argon, 2.5 mL of CH_2Cl_2 , 0.25 mL of MeOH (10:1, v/v) were added, followed by 4.6 mg of $\text{Cu}(\text{OAc})_2 \cdot \text{H}_2\text{O}$ (23 μmol , 20 equiv.). The suspension was heated to reflux in a pre-heated oil-bath (at 50°C) under argon protecting from light. Reaction progress was followed through UV/Vis and TLC, after 1.5h the flask was removed from oil bath to cool down the reaction to room temperature. The resulting dark suspension washed with sat aq. NaHCO_3 (3 x 15 mL) and product mixture extracted into CH_2Cl_2 (ca. 4 x 10 mL) until the organic extracts were colourless. The combined organic extracts were filtered through a plug of dried cotton, and solvents removed under reduced pressure. The residue precipitated in MeOH/ H_2O and dried under H.V. at 50°C for 15 h to obtain 1.7mg (1.03 μmol , 91%) of **3-Cu**.

UV/Vis (in CH_2Cl_2 , c = 4.35 μM): λ_{max} (log ϵ): 724 (4.82), 661 sh (4.19), 545 (4.85), 413 (4.50), 365 (4.45), 253 (4.87).

^1H NMR: Paramagnetic compound.

MALDI-MS (DHB matrix, $\text{C}_{108}\text{H}_{100}\text{N}_4\text{O}_8\text{Cu}$; exact mass = 1643.68); base peak found at m/z (%): 1624.10 (54), 1625.08 (80), 1626.06 (91), 1627.04 (97), 1628.01 (100), 1628.98 (90), 1629.94 (80), 1630.89 (80), 1631.86 (51), 1632.83 (28), 1633.79 (15), 1634.77 (7).

B) *Tetranaphthoquinono Cobalt^(II) Porphyrin (3-Co)*: In an dry 10 mL round bottomed flask, 2 mg (1.26 μmol) of **3-2H** was taken, 2 mL of abs THF and 50 μL of NEt_3 were added, followed by 5.5 mg of anhydrous CoBr_2 (25.1 μmol , 20 equiv.), and reaction was heated at 60°C for 3h. Resulting mixture washed with acidic water (pH 2, 3 x 15 mL) and product extracted into CH_2Cl_2 (ca. 4 x 10 mL), combined organic extracts were filtered through a plug of dried cotton, and solvents removed under reduced pressure. The residue precipitated in MeOH/ H_2O to obtain pure product, which was dried under H.V. at 50°C for 15 h to obtain 1.9mg (1.1 μmol , 87%) of **3-Co**.

UV/Vis (in CH₂Cl₂, c = 3.67 μM): λ_{max} (log ε): 730 (4.67), 661 sh (4.14), 566 (4.65), 418 (4.43), 367 (4.44), 246 (4.90).

¹H NMR: Paramagnetic compound.

MALDI-MS (DHB matrix, C₁₀₈H₁₀₀N₄O₈Co; exact mass = 1639.69); Base peak found at *m/z* (%): 1618.46 (54), 1619.43 (80), 1620.40 (91), 1621.39 (96), 1622.04 (97), 1623.39 (100), 1624.29 (95), 1625.33 (84), 1626.22 (74), 1627.18 (70), 1628.15 (67), 1629.11 (58), 1630.09 (55), 1631.06 (40), 1632.03 (36).

C) Tetranaphthoquinono Porphyrins 3-Zn, 3-Ni, 3-2H: Synthesis and analytical data were reported in [S3, S4].

3-2H: **UV/Vis** (in CH₂Cl₂, c = 38 μM): λ_{max} (log ε): 757 sh (4.33), 707 (4.72), 650 sh (4.31), 554 (5.03), 415 (4.63), 364 (4.40). **¹H NMR** (300 MHz, CDCl₃): -0.48 (s, 2H), 1.54 (s, 72H), 6.97 (s, 8H), 7.90-8.06 (br s, 8H), 8.18 (d, *J* = 1.6 Hz, 8H), 8.28 (t, *J* = 1.6 Hz, 4H). **MS (FAB)** C₁₀₈H₁₀₂N₄O₈: (*m/z*)_{calcd.} = 1582.769 *m/z* (%): 1590.7 (14), 1589.6 (21), 1588.6 (31), 1587.6 (50), 1586.6 (76), 1585.6 (99), 1584.6 (100), 1583.6 (73, [M+H]⁺), 1582.6 (61, M⁺), 1581.6 (16), 1580.5 (8).

MALDI-MS (DHB matrix, C₁₀₈H₁₀₂N₄O₈; exact mass = 1582.769); base peak found at *m/z* (%): 1572.68 (17), 1571.71 (44), 1570.74 (76), 1569.77 (100), 1568.79 (92), 1567.82 (86), 1566.83 (56), 1565.84 (46), 1564.85 (28), 1563.87 (19).

3-Ni: **UV/Vis** (in CH₂Cl₂, c = 10.4 μM): λ_{max} (log ε): 722.5 (4.89), 662 sh (4.22), 533.5 (4.87), 458 sh (4.35), 396 (4.49), 369 (4.47), 302.5 (4.55), 245 (4.89). **¹H NMR** (300 MHz, CDCl₃): 1.44 (s, 72H), 6.94 (s, 8H), 7.77 (d, *J* = 1.7 Hz, 8H), 7.83 (s, 8H), 8.15 (t, *J* = 1.7 Hz, 4H). **MS (FAB)** C₁₀₈H₁₀₀N₄O₈Ni: (*m/z*)_{calcd.} = 1638.689, *m/z* (%): 1646.4 (25), 1645.4 (26), 1644.4 (39),

1643.5 (52), 1642.5 (87), 1641.5 (87), 1640.5 (94), 1639.5 (100, [M+H]⁺), 1638.5 (25, M⁺), 1637.4 (23).

3-Zn: UV/Vis (CH₂Cl₂, *c* = 9.71 μM): λ_{max} (log ε): 725 (4.90), 668 sh (4.29), 555 (4.95), 453.5 sh (4.52), 418 (4.66), 365 (4.53), 325 (4.39), 254 (4.99). ¹H NMR (300 MHz, in CDCl₃): 1.54 (s, 72H), 6.97 (s, 8H), 7.97 (s, 8H), 8.11 (br s, 8H), 8.33 (br s, 4H). FAB MS (C₁₀₈H₁₀₀N₄O₈Zn; exact mass = 1644.683). *m/z* (%): 1651.8 (32), 1650.8 (48), 1649.8 (71), 1648.8 (86), 1647.8 (100) 1646.8 (95), 1645.8 (79, [M+H]⁺), 1644.8 (61, M⁺).

X-ray structure analysis of 3-Zn: See reference [S3] (CCDC No. 699277)

6. UV/Vis Spectra

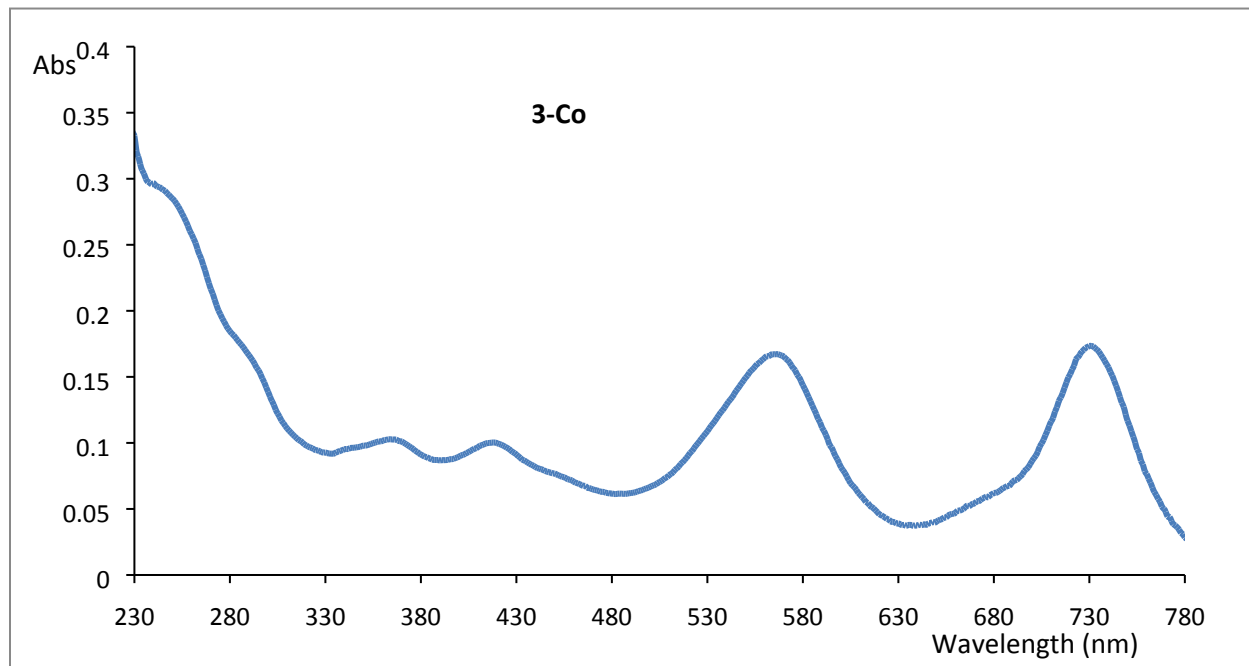


Fig. S1: UV/Vis-spectra of **3-Co** in CH_2Cl_2 (Conc. = $3.366 \mu\text{M}$ in CH_2Cl_2).

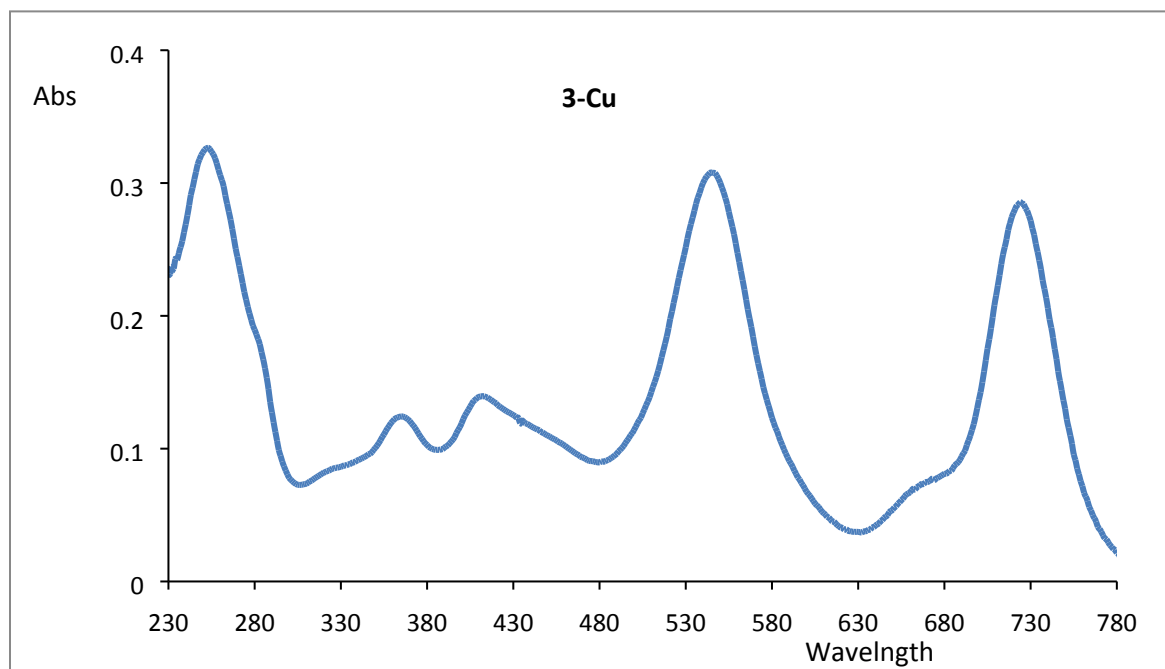


Fig. S2: UV/Vis-spectra of **3-Cu** in CH_2Cl_2 (Conc. = $4.356 \mu\text{M}$ in CH_2Cl_2).

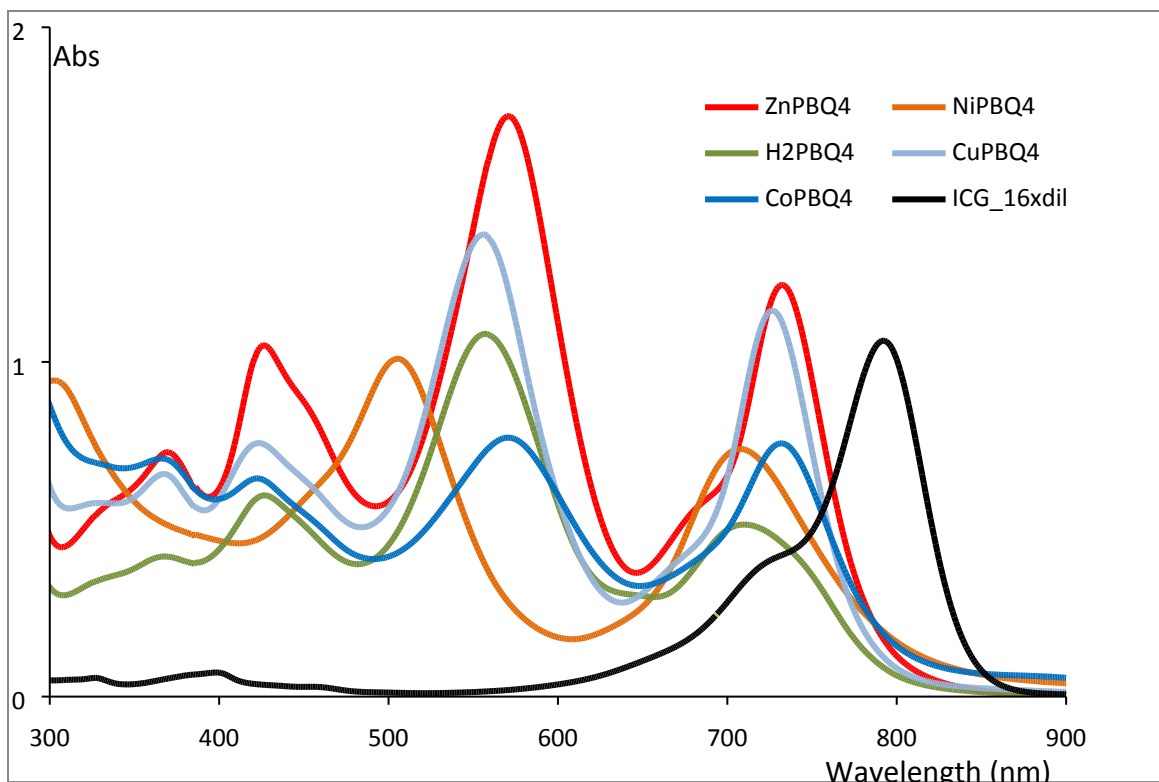


Fig S3: Overlay of UV/Vis-absorption spectra of naphthquinonoporphyrins (**3-M**) and ICG in DMF (concentrations: 16 μM of **3-2H** ($\text{H}_2\text{P}(\text{BQ})_4$); 23 μM of **3-Zn**, ($\text{ZnP}(\text{BQ})_4$); 26 μM of **3-Cu**, ($\text{CuP}(\text{BQ})_4$); 31 μM of **3-Ni**, ($\text{NiP}(\text{BQ})_4$); 29 μM **3-Co** ($\text{CoP}(\text{BQ})_4$); 11 μM of ICG).

7. Fluorescence spectra of **3-Zn**

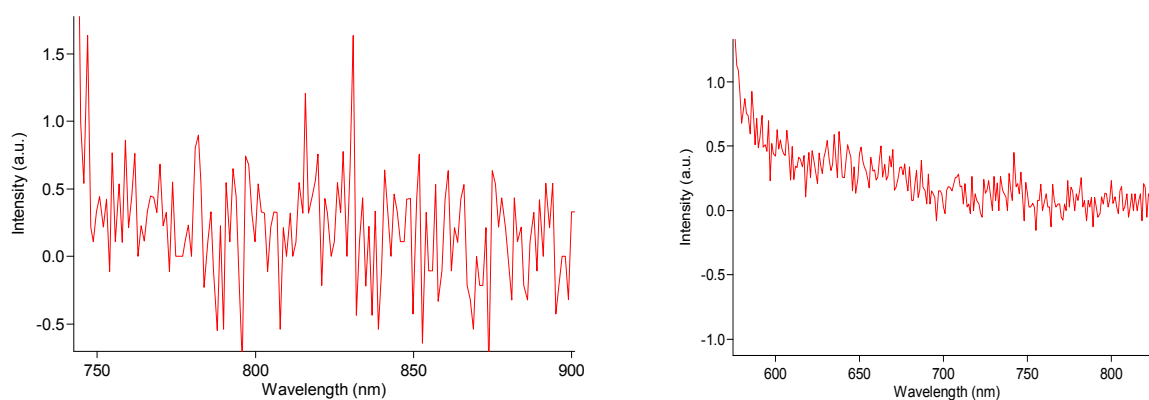


Fig S4: Fluorescence emission spectra of **3-Zn** (12 μM , 10% MeOH in CH_2Cl_2): Left at $\lambda_{\text{exc}} = 736$ nm and right at $\lambda_{\text{exc}} = 567$ nm.

8. Phantom design images



Fig S5: Images of the blood vessel mimicking water-chamber phantom used in this manuscript.

Chicken muscle phantom Imaging:



Fig S6: PAI of the chicken muscle phantom. A DMF solution containing the dyes was injected into the bottom layer of the chicken muscle, and thin layers of chicken muscle were placed on the top to generate an additional depth for the photoacoustic imaging.

9. PA spectroscopy

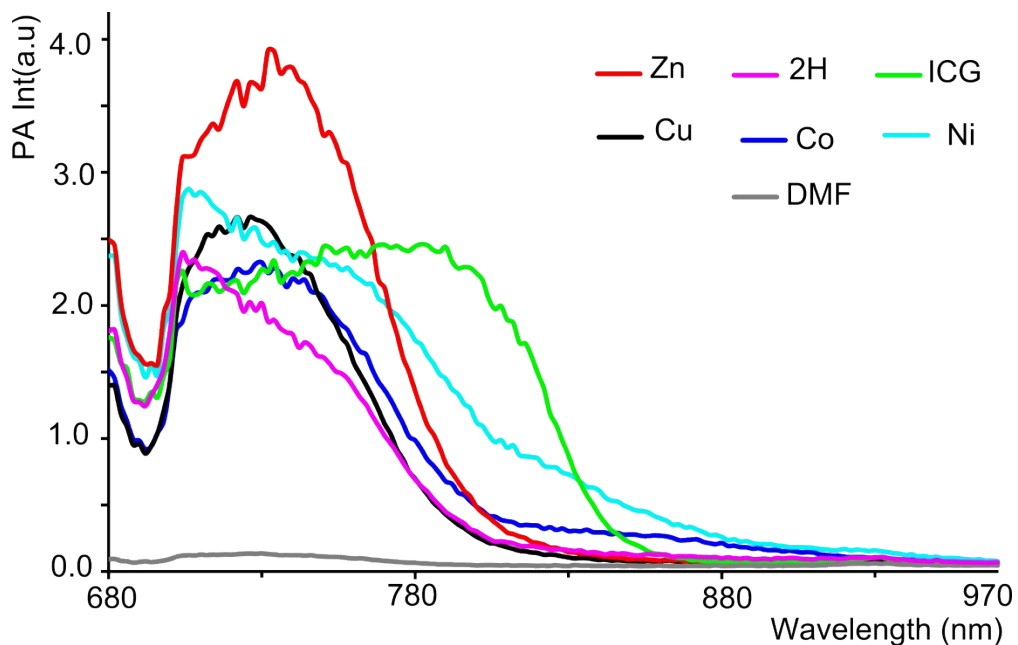


Fig S7: PA spectroscopy of the ‘black’ porphyrins **3-M** and ICG (in DMF, (concentrations: 63 μM of **3-2H**; 91 μM of **3-Zn**; 124 μM of **3-Ni**; 106 μM of **3-Cu**; 115 μM **3-Co**; 181 μM of ICG).

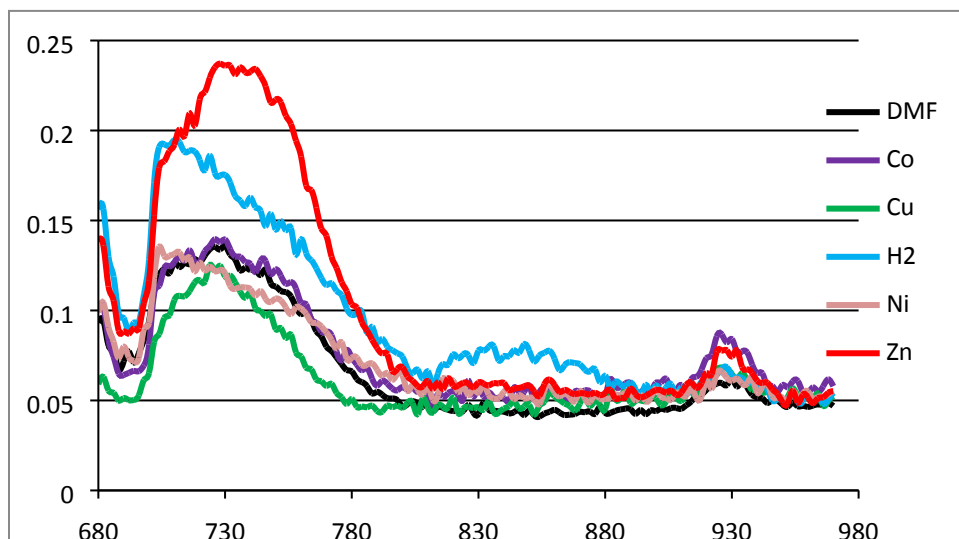


Fig S8: In DMF 20x diluted solutions of **3-M** PA spectroscopy (conc. = 3.2 μM of **3-2H**; 4.6 μM of **3-Zn**; 6.2 μM of **3-Ni**; 5.3 μM of **3-Cu**; 5.8 μM **3-Co**; 9 μM of ICG).

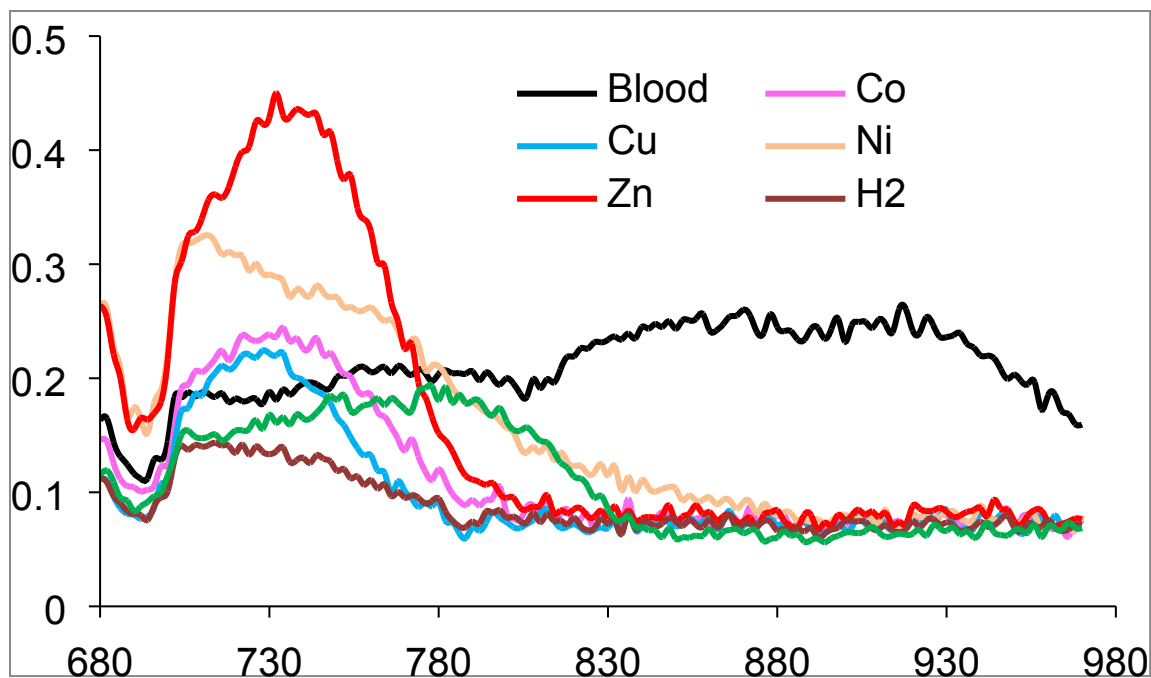


Fig S9: PA spectroscopy in 4x whole blood dilutions (conc. = 15.7 μM of **3-2H**; 22.8 μM of **3-Zn**; 31 μM of **3-Ni**; 26.5 μM of **3-Cu**; 28.8 μM **3-Co**; 45.2 μM of ICG).

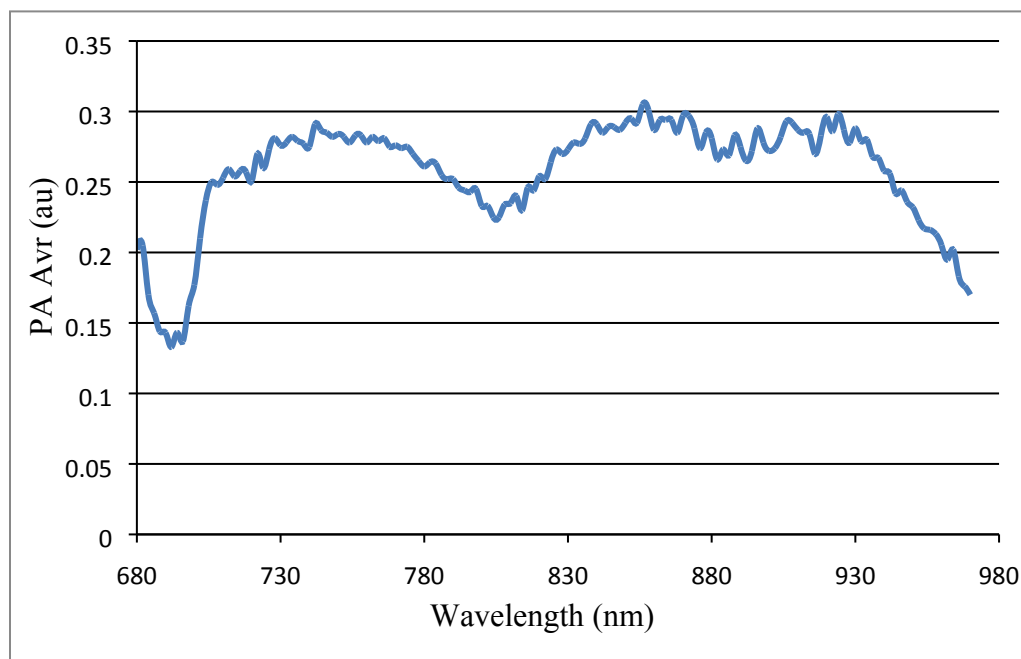


Fig S10: PA spectroscopy of whole blood (Swine, injected into a tube phantom).

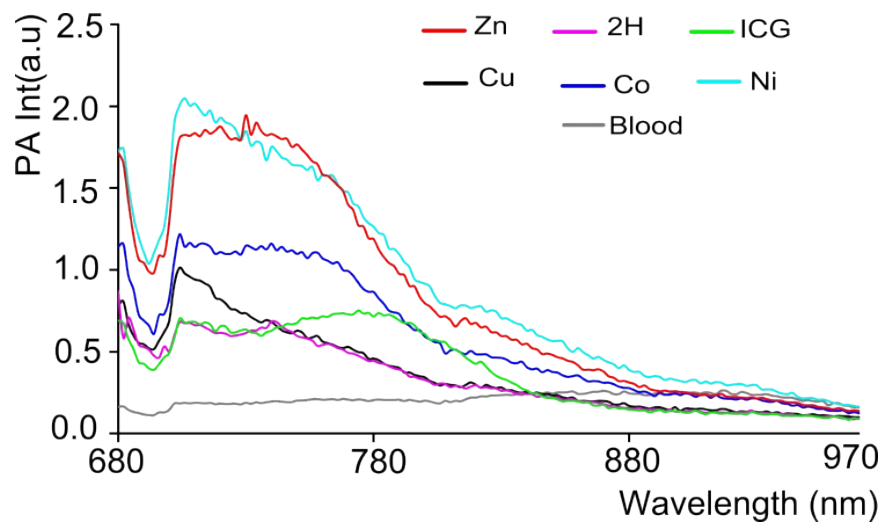


Fig S11: Blood PA Avr un-subtracted PA spectroscopy of **3-Ms** in whole blood, Conc. in μM , **3-2H** (42), **3-Co** (76.6), **3-Cu** (70.6), **3-Ni** (82.6), **3-Zn** (60.6), and ICG (120.6).

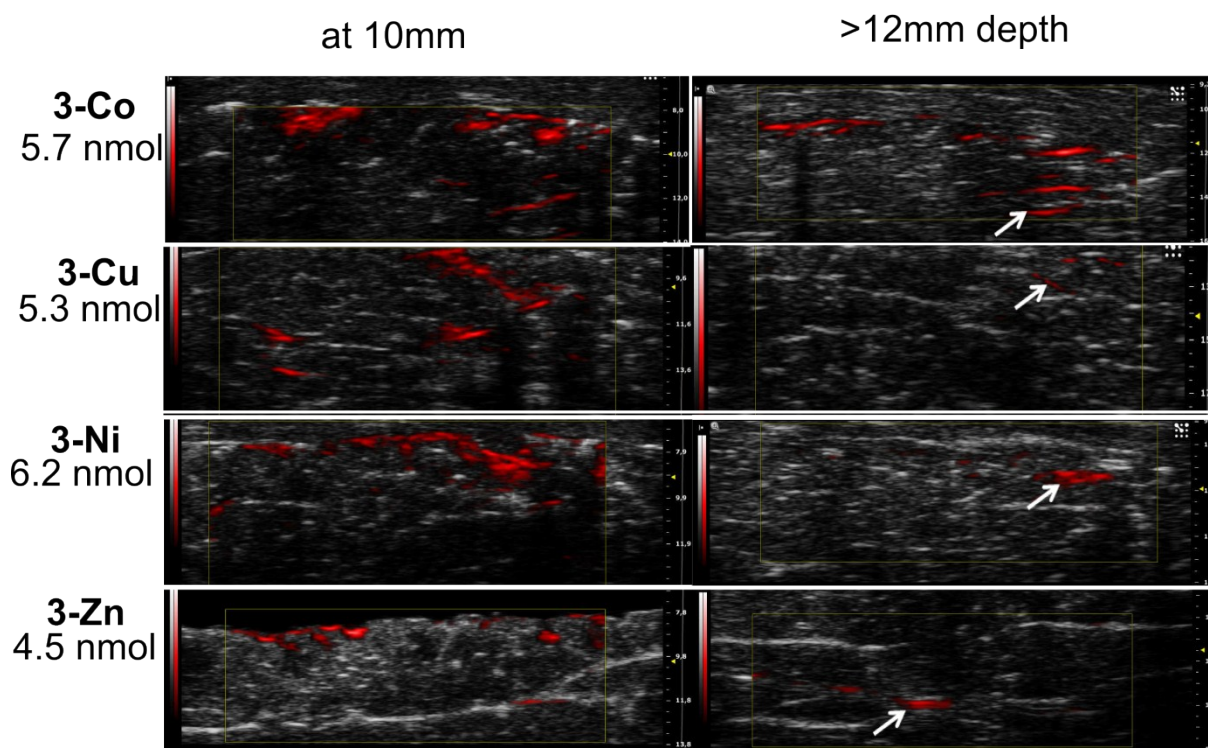
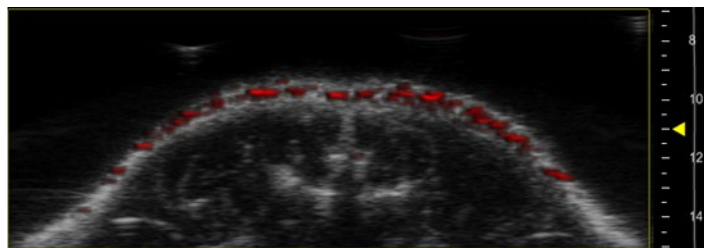


Fig S12: PA images of **3-M** in chicken muscle phantom (Ni: 720 nm, Cu: 726 nm, Co and Zn: 730nm).

Blank



3-Zn
3.34 nmol
left: 1 mm depth
right: 3 mm depth

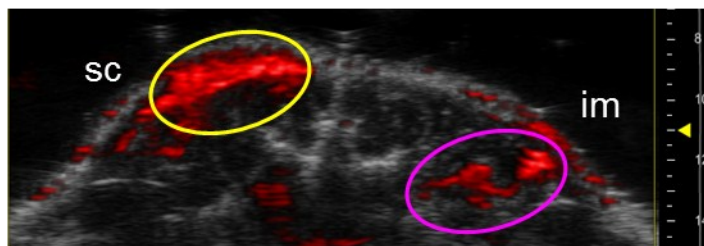


Fig S13: PA snapshot image (at 720nm) of **3-Zn** injected dead mouse at different depths (s.c = subcutaneous, 1 mm deeper, im = intramuscular, 3 mm deeper).

10. Stability of 3-Zn in 10% fetal calf serum (FCS) in PBS buffer

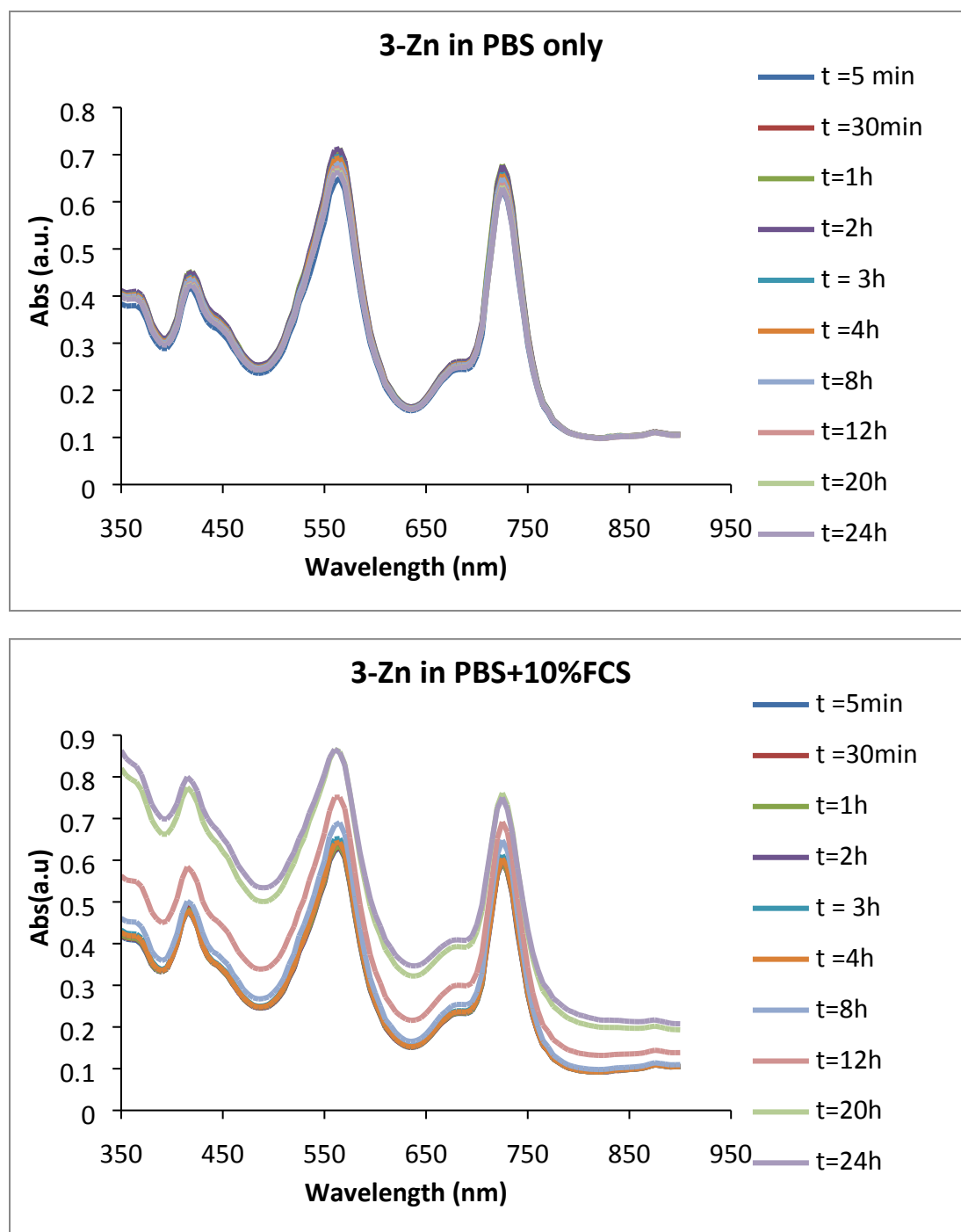


Fig S14: UV-Vis spectroscopy of **3-Zn**:cremophore EL in PBS (Top), and of **3-Zn**:cremophore in 10% FCS contained PBS (bottom) (average of 3 measurements; conc.: 15 μ L of 1mM of **3-Zn** solution to 200 μ L volume per well) (over 24h, some solution evaporation has caused a little shift in maxima of the 2nd spectrum).

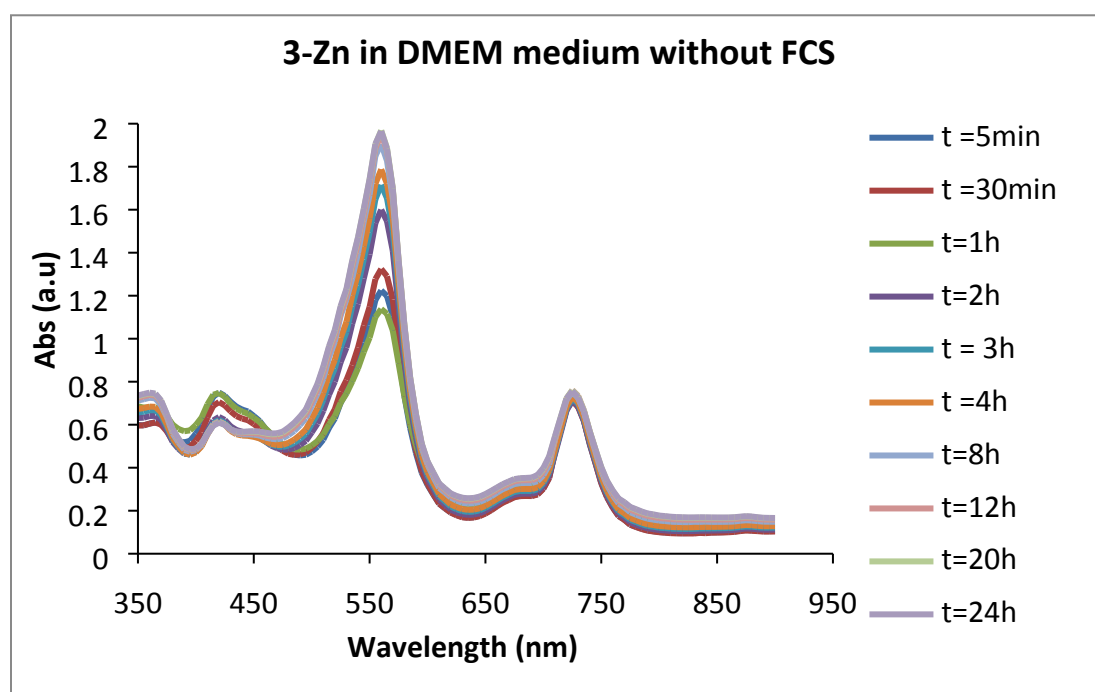
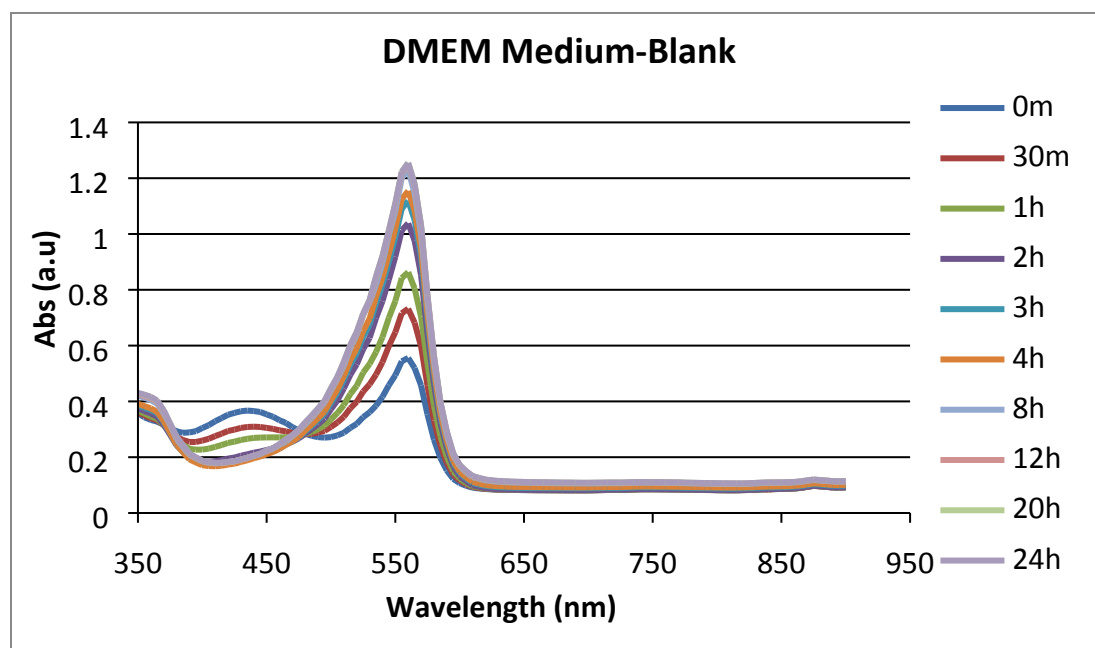


Fig S15: UV-Vis spectroscopy of **3-Zn:cremophore** in DMEM medium (Top), and of **3-Zn:cremophore** in 10%FCS contained DMEM medium (bottom) (average of 3 measurements, conc: 15 μ L of 1mM of **3-Zn** solution volume in well: 200 μ L; i.e. 75 nmol/ml).

11. Stability of 3-Zn to excess of free thiol (N-Ac-Cys-OMe): In a HPLC vial, 0.3 mg of **3-Zn** in ethylacetate (1 ml) was taken, added 2 mg of N-acetylated cysteine methylester (Ac-Cys-OMe, Sigma Aldrich), and reaction was followed by injecting 5 μ L of the mixture at different time points in supercritical fluid chromatography (SFC, column: Kromasil-Si-60, method: 4ml_10min_35ml_gradient).

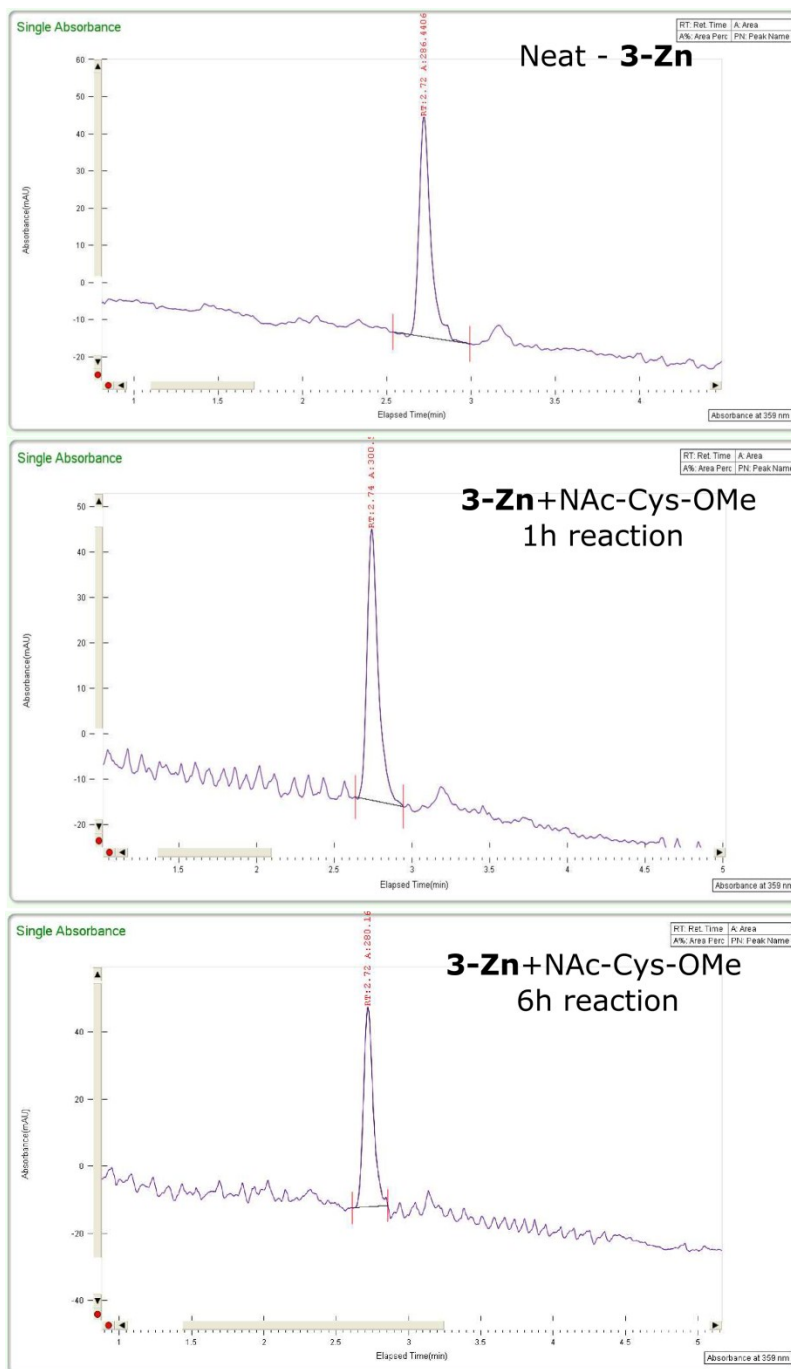


Fig S16: Supercritical fluid chromatography (SFC-) traces of **3-Zn** reaction with N-acetyl-cysteine-methylester (1h, 6h) (Similar retention times can be seen in each chromatogram).

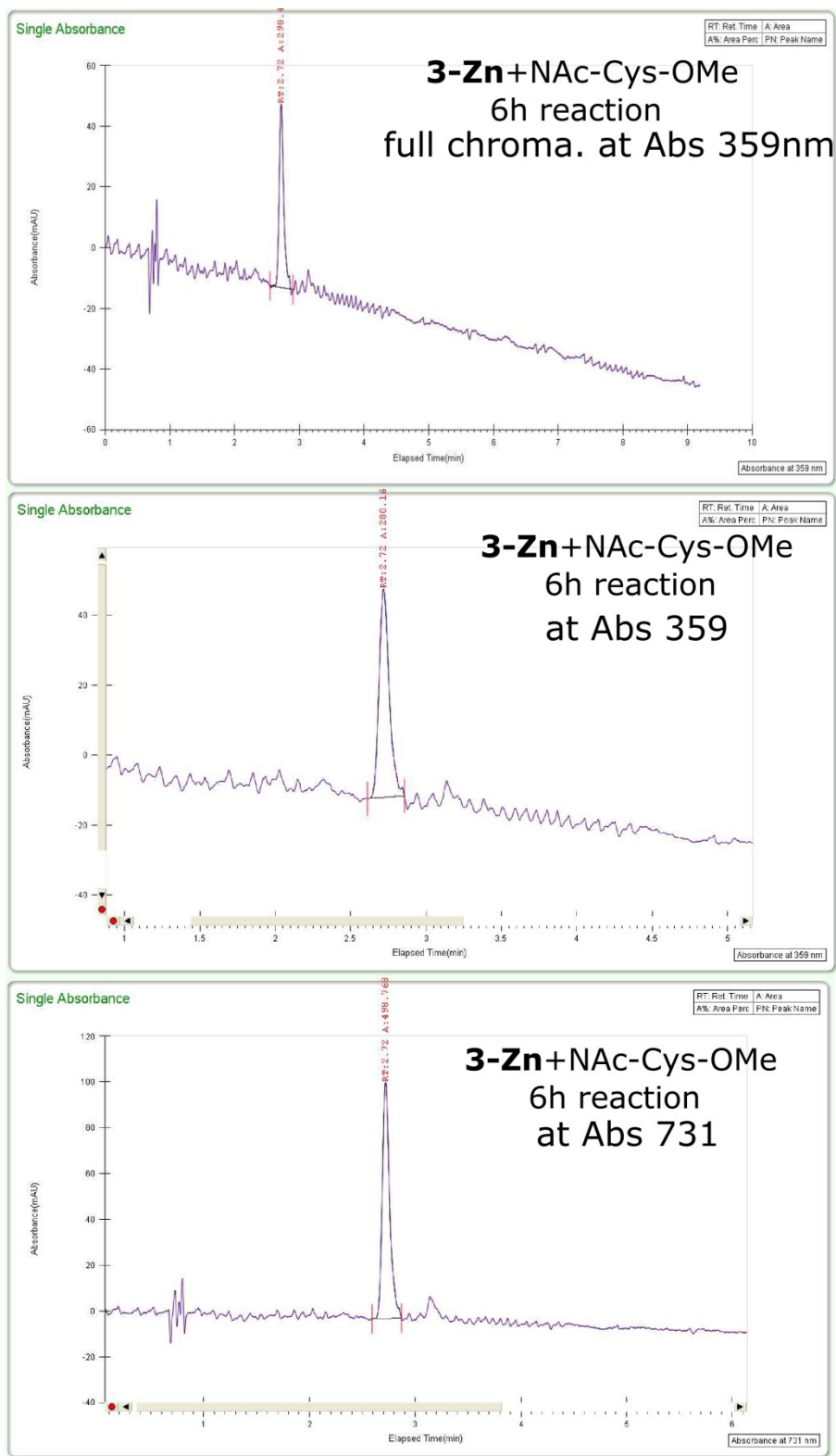


Fig S17: SFC-trace of **3-Zn** reaction with N-acetyl-cysteine-methylester after 6h (in 10 min elution at Absorbance at 359 and at 731 nm).

12. Mass spectra

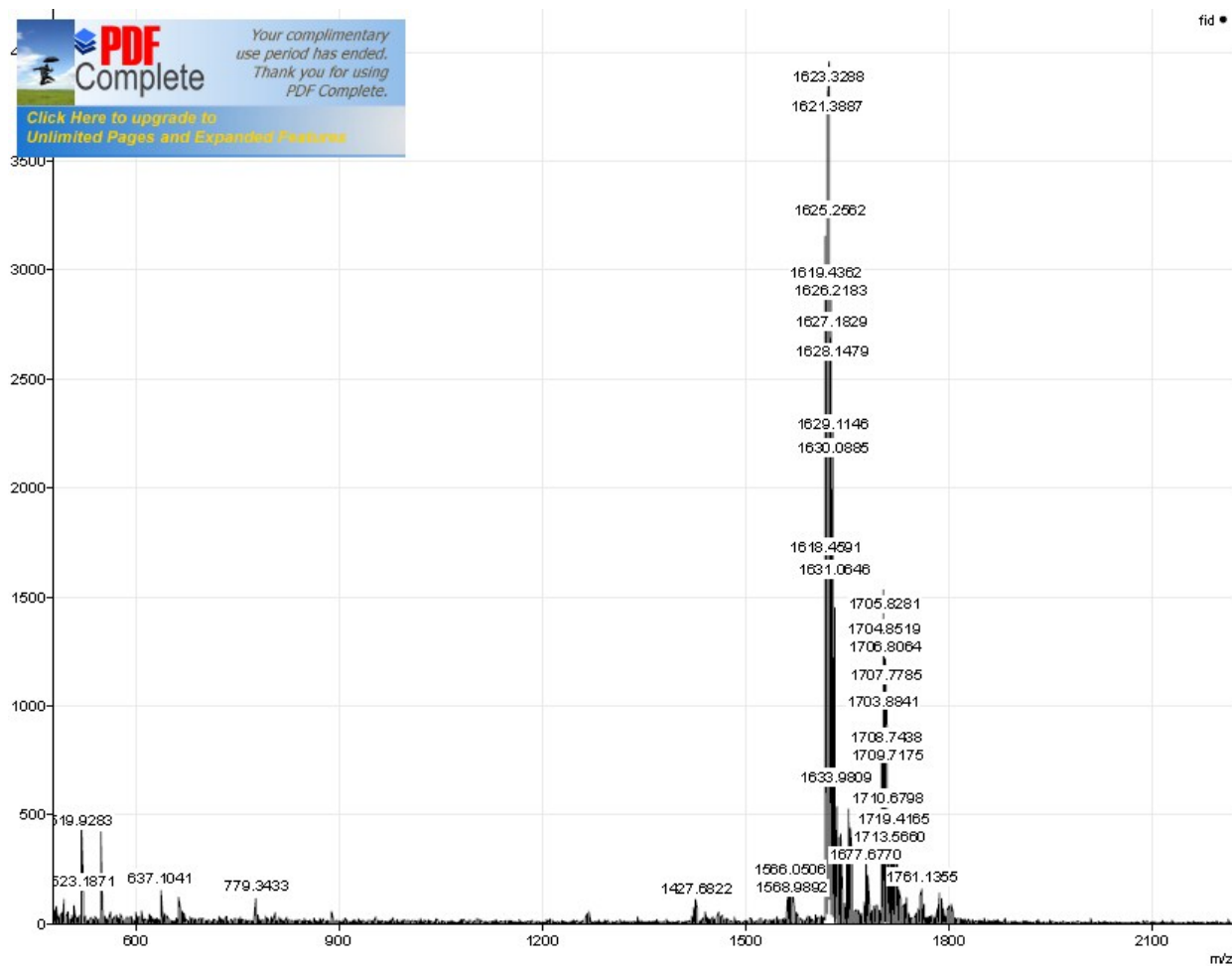


Fig S18: MALDI (in DHB) spectra of **3-Co**.

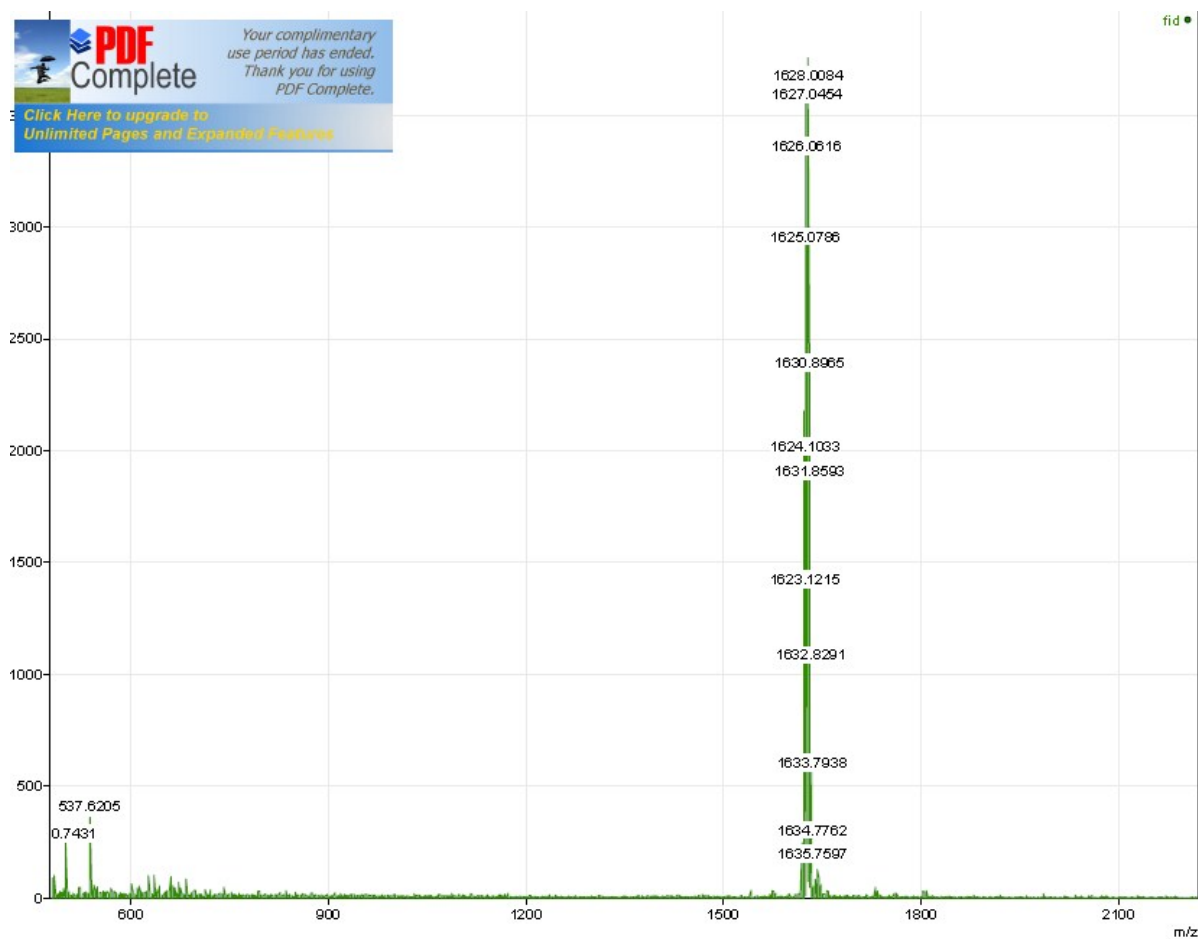


Fig S19: MALDI (in DHB) of **3-Cu**.

13. References:

- S1. N.C. Burton, M. Patel, S. Morscher et al. *Neuroimage* **2013**; 65, 522.
- S2. V. Neuschmelting, H. Lockau, V. Ntziachristos, J. Grimm, *Radiology*. **2016**; 280,137
- S3. S. Banala, T. Rühl, P. Sintic, K. Wurst, B. Kräutler, *Angew. Chem. Int. Ed* **2009**, 48, 599.
- S4. S. Banala, K. Wurst, B. Kräutler, *ChemPlusChem* **2016**, 81, 477.